ELSEVIER

Solar Energy Materials & Solar Cells 75 (2003) 243–251

Solar Energy Materials & Solar Cells

www.elsevier.com/locate/solmat

Quantification of losses in thin-film polycrystalline solar cells

James R. Sites

Physics Department, Colorado State University, Ft. Collins, Colorado, 80523, USA

Abstract

Comparison of measured solar-cell parameters with calculations for ideal cells is a powerful tool to assist fundamental understanding and to focus on the most effective fabrication procedures. The emphasis here will be on quantitative separation of individual loss mechanisms in polycrystalline thin-film cells based on CdTe, $CuInSe_2$ (CIS), and related alloys such as $CuIn_{1-x}Ga_xSe_2$ (CIGS). Several techniques to facilitate separation of losses are described. © 2002 Published by Elsevier Science B.V.

Keywords: Photons; Diodes; CdTe; $CuIn_{1-x}Ga_xSe_2$; Crystallites; Thin films

1. Photon accounting

There are a variety of possible optical losses before photons reach a solar cell's absorber, and there are additional losses from non-radiative recombination or from photons exiting the absorber. Fig. 1 is one example of the fraction of photons of each wavelength that contributed to a cell's short-circuit current density and the fractions that were lost in each of several ways [1]. The cell shown is an early Solar Cells, Inc. CdTe cell that had significantly larger photon losses than those currently seen.

To quantify the photon losses, the measured quantum efficiency (QE) is multiplied by the light spectrum, in units of photons/cm^2 nm, integrated over wavelength, in units of nm, and multiplied by the unit electronic charge to get the measured current density. For comparison, the maximum current density is assumed to be the same calculation with unity QE up to the band-gap cutoff wavelength.

The optical measurements shown are the reflection from the cell, the absorption of the glass superstrate, the absorption of the SnO_2 conductive contact, and the absorption of the fairly thick CdS window. The absorptions were deduced from reflection and transmission of partial cells terminated after each layer. The remaining

0927-0248/03/$ - see front matter © 2002 Published by Elsevier Science B.V.
PII: S0927-0248(02)00166-6

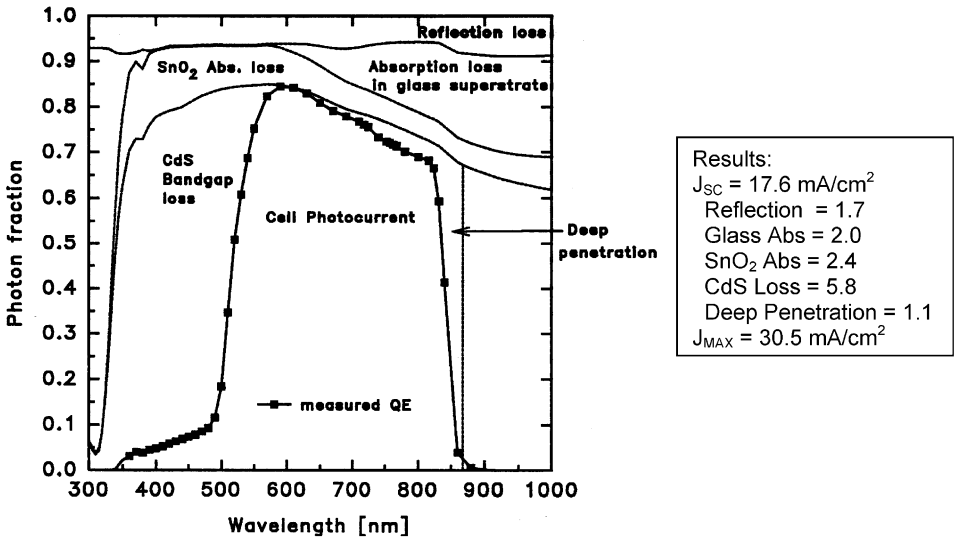

Fig. 1. Photon accounting for a CdTe solar cell [1].

region approaching the band gap is assumed to be due to photons that penetrated too deeply for complete collection. Integration of these areas, again weighted by the spectrum, gives the current-density loss for each. These losses are listed in the inset to Fig. 1 for the standard global AM1.5 spectrum [2] normalized to 100 mW/cm^2. The sum of the losses is the difference between the measured and maximum current densities.

The inset tells us quantitatively that considerable current enhancement is possible by going to a thinner CdS window, some is possible with a different glass or improved SnO_2 process, but not so much from an anti-reflection coating and only a small amount from better collection of the deeply penetrating photons. The larger loss issues have been addressed, and CdTe photocurrents as large as 26.2 mA/cm^2 have been produced [3].

2. Resistive and diode-quality factor losses

Losses due to shunting can generally be deduced from the slope of the current–voltage curve near zero bias for an illuminated cell. The fractional loss in current at maximum power J_{MP}, and hence the fractional loss in efficiency, is approximately the maximum power voltage V_{MP} divided by J_{MP} and the shunt resistance r.

The experimental determination of r is complicated if there is a voltage dependence to the photocurrent J_L. In that case, the slope of the current–voltage curve near zero bias is not constant, and hence a single-parameter correction is not sufficient. There are, however, techniques to handle the combined effects of shunting

and $J_L(V)$ [4]. The reduction in J_{MP} due to $J_L(V)$ can also be calculated. It has been estimated to be about 2% for typical CIS cells, and about 1% for CdTe cells, which generally have a wider depletion region [5].

A cell's effective series resistance R can usually be separated from its diode quality factor A by linearizing the diode equation and plotting dV/dJ vs. $(J + J_L)^{-1}$ [6]. Such plots for a 10% CdTe cell, both light and dark, are shown in Fig. 2. The fact that the slopes and intercepts are significantly different with and without light strongly cautions against analysis techniques that assume illumination-independent parameters.

The y-intercepts in Fig. 2, effectively the voltage–current slopes extrapolated to infinite current, are the light and dark series resistances of the cell. For this cell, the light/dark difference in R is quite large: $2.4\,\Omega\,cm^2$ in the light vs. $54\,\Omega\,cm^2$ in the dark. For both light and dark, the uncertainty is about 5%.

The slopes in Fig. 2 are the diode exponentials in voltage units, $V_O = Ak_BT$. The resulting A values are 1.6 in the light and 2.4 in the dark, again with an uncertainty of about 5%. If solar-cell data is less clean than that used for Fig. 2, a judicious selection of which data points to use is important, and generally the range between V_{MP} and V_{OC} is emphasized.

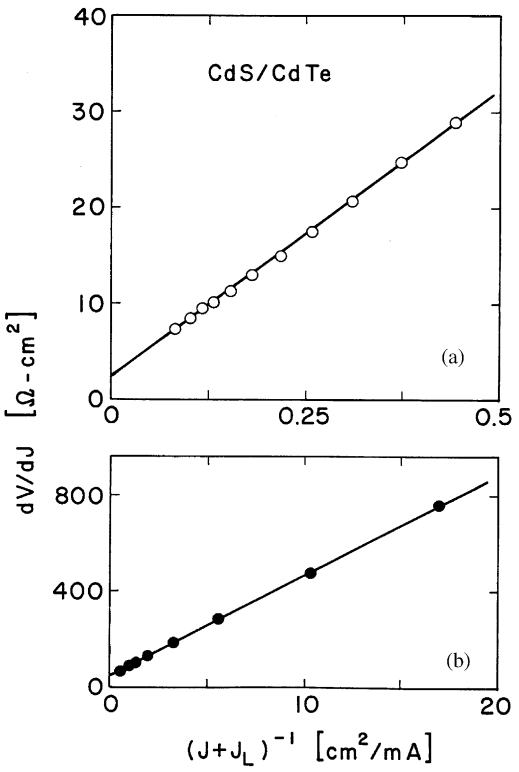

Fig. 2. Differential plot to separate R and A [6]. Light data is shown in (a), dark in (b).

The conversion of a cell's series resistance to an efficiency loss is similar to the conversion of a shunting loss. The fractional loss in voltage or efficiency is approximately equal to $J_{MP}R/V_{OC}$. The efficiency reduction due to an A-value greater than one is also relatively straightforward and will be discussed in the following section.

In most cases, deviations from the diode equation can be readily identified from non-linear parts of the dV/dJ plots. Examples of two such deviations for a CIS cell under illumination are shown in Fig. 3. This cell had a low shunting resistance r, but the quantity plotted on the horizontal axis can be modified to again give a linear relationship over much of the current range for the two temperatures shown. The open symbols assume $r = \infty$, and the arrows to the closed symbols show the correction for the measured value of r.

The second deviation in Fig. 3 is only seen in the low-temperature data. In this case, the cell's forward current is limited due to a contact barrier, which will be discussed in more detail below. The effect, however, appears as a rapid upturn for low values of inverse current. The rest of the curve, which is largely unaffected by the contact barrier, gives reliable values for R and A, but the need for judicious selection of the data range is dramatically illustrated.

3. Excess forward current

The diode quality factor of a cell is a key indicator of excess forward current, which can often be attributed to electron–hole recombination through traps in the

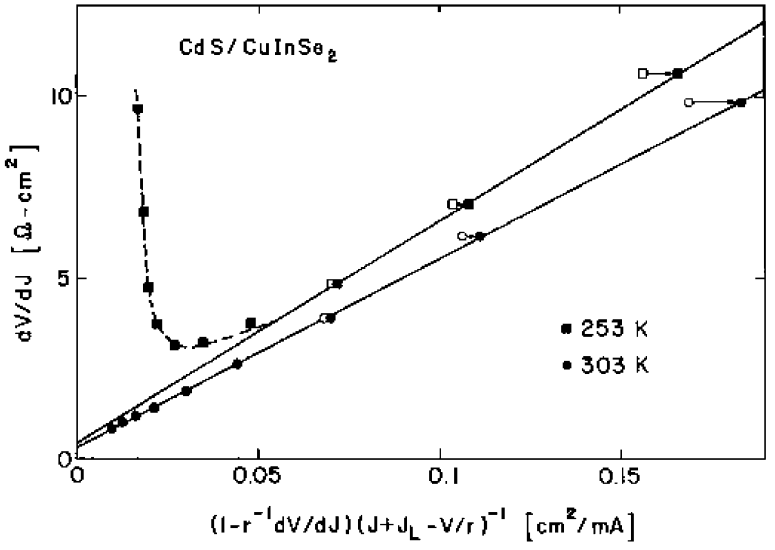

Fig. 3. dV/dJ plots with non-standard features [6].

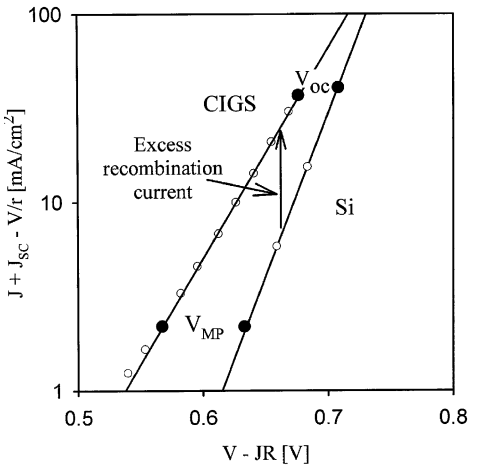

Fig. 4. Comparison of Si and CIGS $J-V$ curves.

junction region. Excess forward current implies a reduced operating voltage. This effect is illustrated in Fig. 4, which shows a plot of the forward current density, defined as the experimental curve shifted by the short-circuit current density, on an exponential scale. The two curves shown are from a high quality Si cell with an A-factor near 1.0 and a high-quality CIGS cell of similar band gap, as determined from the QE cutoff, with A near 1.5. The curves for both cells have been corrected for modest series resistances and shunting.

Fig. 4 shows that V_{OC} for the CIGS cell is smaller than that for the crystalline Si cell by about 30 mV. At V_{MP}, however, due to the different slopes of the two curves, the voltage difference has increased to 65 mV. The additional 35 mV is $k_B T$ times the difference in A-factors (0.5) times the natural log of $J_{SC}/(J + J_{SC})$, about 2.8 in this case.

A more physical way to look at Fig. 4 is in terms of the excess forward recombination current of the CIGS cell, which is illustrated by the vertical arrow. The ratio of the forward currents for the two cells shown varies with voltage, but it is near five at V_{MP}. For lower quality cells, however, the ratio can easily be a factor of 100.

4. Secondary barriers

It is not uncommon for thin-film solar cells to have circuit components in addition to the single diode junction plus single-parameter resistances. The more dramatic deviations of $J-V$ curves from a diode-like appearance are generally due to the existence of an unintended secondary barrier within the layered structure.

Metallic contacts to semiconductors, especially those to relatively high band-gap p-type materials, often form barriers to carrier transport. A simple circuit model

shown in the upper part of Fig. 5 with series-connected diodes of opposing polarities can give a reasonable fit to experimental data. The primary solar-cell diode is on the left, and the secondary back-contact diode is on the right. The single parameter needed to calculate the $J-V$ curve for a range of temperatures is the contact-barrier energy. The fit of this model to experimental data is quite good for the CdTe cell shown in the lower part of Fig. 5 [1].

The primary effect of the back-contact barrier is to limit the current in the first quadrant, when the primary diode is forward biased and the contact diode is reverse biased. This feature often referred to as rollover. As seen in Fig. 5, it becomes progressively more pronounced as the temperature is lowered. The effect on cell performance, seen in the fourth quadrant, however, is relatively modest even.

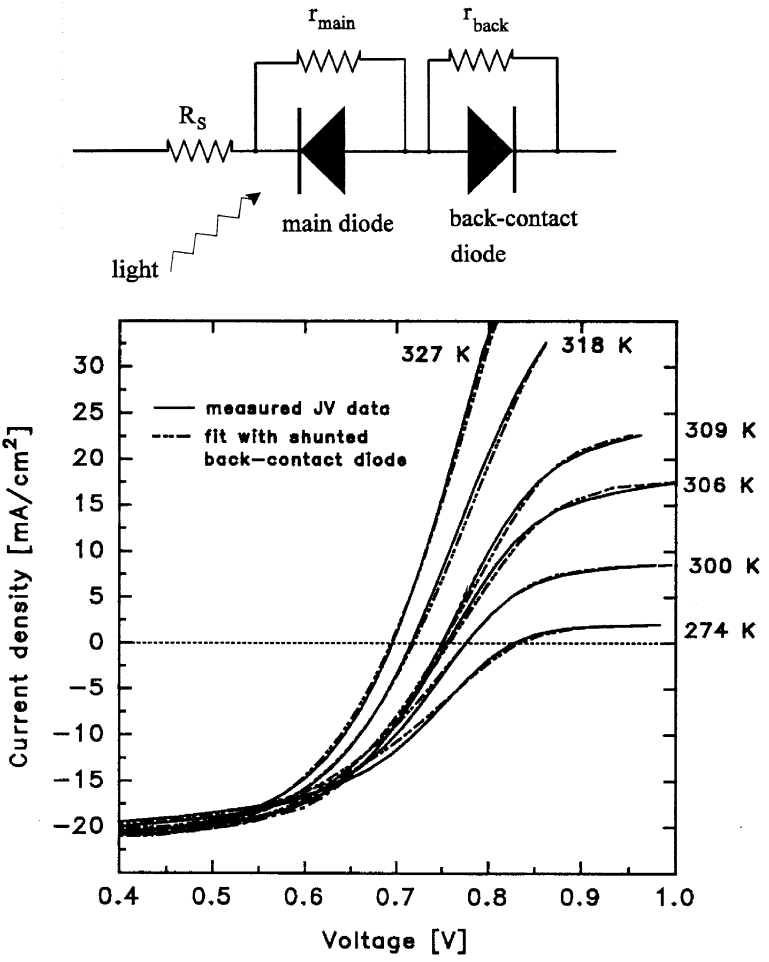

Fig. 5. Effect of back-contact barrier [1].

The model pictured above does assume that the two diodes are independent circuit elements. If the depletion width of a cell is large compared to its thickness, however, this assumption fails, the built-in potential is effectively reduced, and the back contact can have a much more dramatic impact on the cell's $J-V$ curves [7]. This is a particular concern for CdTe cells, where the absorber carrier density is typically low and the depletion region wide.

A secondary barrier in the region of the primary diode due to band offsets is also possible. The offset in the conduction band between CdS window and CIS absorber has been calculated with reasonable accuracy [8]. The impact of this barrier on cell performance depends on the thickness of the CdS, and the carrier densities of the window and absorber. Fig. 6 below shows the effect on $J-V$ curves in one case where the carrier density in the CdS window was altered by short wavelength photons [9].

The $J-V$ curves in Fig. 6 were measured with "red" illumination consisting only of photons with energy below the CdS band gap. The illuminated curve taken without recent exposure to higher energy photons has a "kink", which is the signature of two diodes of the same polarity which are connected in series. The corresponding dark curve also fits the two-diode model. Curves taken just after exposure to white-light illumination or monochromic light above the CdS band gap have a standard solar-cell appearance. These "normal" curves gradually revert to the

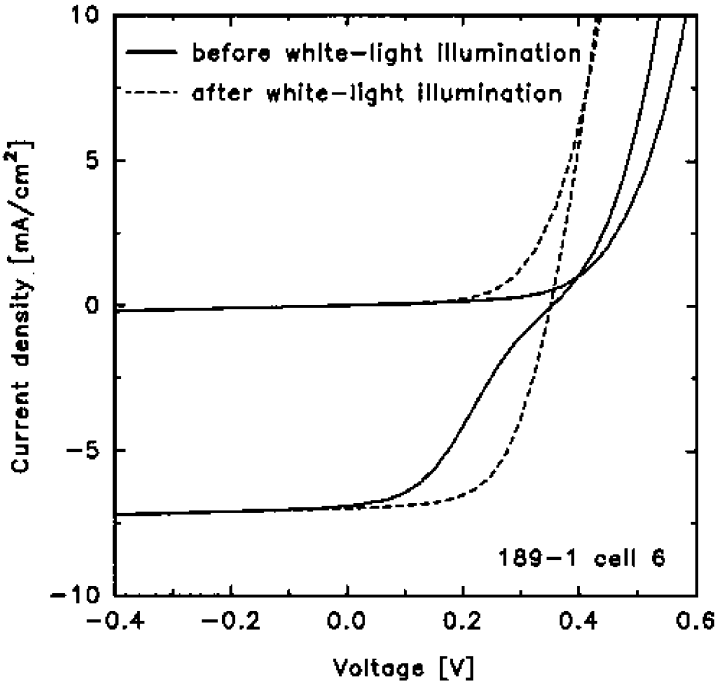

Fig. 6. $J-V$ "kink" due to conduction band offset [9].

original "red-light" curves if not exposed to more high-energy photons. Agreement of calculation and experiment is again quite good.

5. Local variations

Polycrystallinity is inherently non-uniform, and one cannot assume that average measurements made on whole cells apply evenly to microscopic areas. Fig. 7 shows local-area photocurrent maps of two CdTe cells under laser illumination, one made with the $CdCl_2$ treatment often used for high-efficiency cells. Without this process step, photocurrents are 30% lower in some areas than others.

In some cases, such as the one shown in Fig. 7, the regions of reduced photocurrent are due primarily to local areas of high resistance, while in others they are due to reduced diode barriers. The two possibilities are separable by varying the cell bias and the local laser intensity [10].

6. Discussion

Quantitative evaluation of losses in polycrystalline thin-film solar cells allows systematic comparisons, both to other cells and to ideal targets. Specific losses,

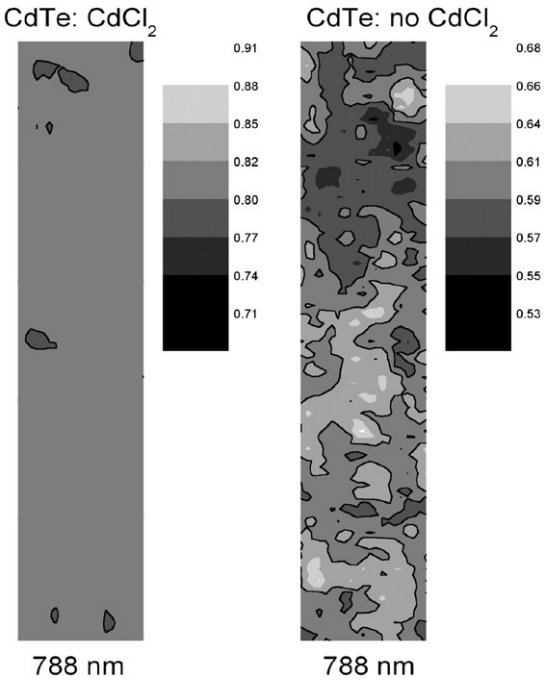

Fig. 7. Photocurrent maps. Illumination is one sun; scale is $10 \times 50\,\mu m^2$ [10].

associated to varying degrees with specific physical mechanisms, considerably expand the information given by the standard parameter breakdown into current and voltage intercepts plus fill-factor. There are, however, a number of possible pitfalls in the process, and there are reasonable quality cells that have features not easily defined by a closed-form approach. Hence, at least for the foreseeable future, loss analysis will consist of the application of increasingly sophisticated techniques that are critically examined at each step by an experienced observer.

Acknowledgements

The author is grateful to several colleagues who have worked with him at Colorado State University: Peter Mauk, Ingrid Eisgruber, Gunther Stollwerck, Nancy Liu, Jennifer Granata, Jason Hiltner, Pam Johnson, Alex Pudov, and Caroline Jenkins. The work has been supported by the US National Renewable Energy Laboratory.

References

[1] G. Stollwerck, Quantitative separation of photon and back-contact losses in CdTe solar cells, M.S. Thesis, Colorado State University, 1995.
[2] R. Hulstrom, R. Bird, C. Riordan, Standard solar spectra, Sol. Cells 15 (1985) 365–381.
[3] S.P. Albright, B. Ackerman, R.R. Chamberlin, J.F. Jordan, Status of CdTe development at Photon Energy, Inc, APS Conf. Proc 268 (1992) 17–32.
[4] J.E. Phillips, J. Titus,D. Hoffman, Determining the voltage dependence of the light current in $CuInSe_2$ solar cells, Proceedings of the 26th IEEE Photovoltaics Specialists Conference, 1997, pp. 463–466.
[5] X.X. Liu, J.R. Sites, Variation of solar-cell collection efficiency with depletion width, J. Appl. Phys. 75 (1994) 572–576.
[6] J.R. Sites, P.H. Mauk, Diode quality factor determination for solar cells, Sol. Cells 27 (1989) 411–417.
[7] T.J. McMahon, A.L. Fahrenbruch, Insights into the nonideal behavior of CdS/CdTe solar cells, Proceedings of the 28th IEEE Photovoltaics Specialists Conference, 2000, pp. 539–542.
[8] S.H. Wei, A. Zunger, Band offsets at the $CdS/CuInSe_2$ junction, Appl. Phys. Lett. 63 (1993) 2549–2551.
[9] I.L. Eisgruber, J.E. Granata, J.R. Sites, J. Hou, J. Kessler, Blue-photon modification of nonstandard diode barrier in $CuInSe_2$ solar cells, Sol. Energy Mater. Sol. Cells 53 (1998) 367–377.
[10] J.F. Hiltner, Investigation of spatial variations in collection efficiency of solar cells, Ph.D. Thesis, Colorado State University, 2001.